

Testing the Effectiveness of Treatment for Cancers for which the Endpoint is Survival Using Bayesian Subgroup Analysis

by

Yueyang Han

B.Sc., University of Waterloo, 2022

Project Submitted in Partial Fulfillment of the
Requirements for the Degree of
Master of Science

in the
Department of Statistics and Actuarial Science
Faculty of Science

© Yueyang Han 2024
SIMON FRASER UNIVERSITY
Spring 2024

Copyright in this work is held by the author. Please ensure that any reproduction or re-use is done in accordance with the relevant national copyright legislation.

Declaration of Committee

Name: Yueyang Han

Degree: Master of Science

Thesis title: Testing the Effectiveness of Treatment for Cancers for which the Endpoint is Survival Using Bayesian Subgroup Analysis

Committee:

Chair: Wei (Becky) Lin
Lecturer, Statistics and Actuarial Science

Haolun Shi
Supervisor
Assistant Professor, Statistics and Actuarial Science

Jiguo Cao
Committee Member
Professor, Statistics and Actuarial Science

Owen Ward
Examiner
Assistant Professor, Statistics and Actuarial Science

Abstract

We propose a basket trial design that tests the effectiveness of a new treatment for several types of cancers where the endpoint is the survival time. During the trial conduct, Bayesian subgroup analysis is conducted to classify the cancer types into different clusters according to both the survival time and the longitudinal biomarker measurements of the patient. Finally, we make Bayesian inferences to decide whether to stop recruiting patients for each cluster early and make conclusions about whether the treatment is effective for each cluster according to the estimated median survival time. The simulation study shows that our proposed method performs better than the independent approach and the Bayesian Hierarchical Modeling (BHM) method in most of the scenarios.

Keywords: Bayesian subgroup analysis; Longitudinal biomarkers; Phase I/II trials; Clinical trials for cancer

Acknowledgements

I would like to express my sincere gratitude to my supervisor Haolun Shi. His support and patience have been very crucial to my academic accomplishments during my master's study. He has a very solid and broad knowledge of statistical theory and its applications in pharmaceutical statistics, which helped me a lot when I conducted this research. I deeply thank him for helping me overcome the difficulties that I faced when I wrote this thesis. I will never forget his warmth and kindness. I am also thankful to Dr. Jiguo Cao, Dr. Owen Ward, and Dr. Becky Lin for reading my thesis and providing insightful suggestions. My gratitude also goes to all other faculty members and sta

Table of Contents

List of Tables

Table 4.1	Results of the main simulation study which compares the performance of the proposed model with the independent approach and the BHM method. This table shows the early stopping rate, rejection rate, and sample size under ν simulation scenarios.	12
-----------	---	----

List of Figures

Figure 3.1	The posterior distribution of the median survival time for cluster 1 at the interim analysis.	8
Figure 3.2	The posterior distribution of the median survival time for cluster 2 at the interim analysis.	9
Figure 3.3	The posterior distribution of the median survival time for cluster 1 at the end of the trial.	9
Figure 4.1	Mean biomarker measurement. The solid and dashed line represents the mean biomarker measurement for the effective group and the ineffective group, respectively.	11
Figure 4.2	Early stopping rate in the main simulation study. The red, green, and blue bars represent the BHM method, the independent approach, and the proposed method, respectively. Scenarios A1 to A5 vary regarding the number of effective/ineffective treatments.	13
Figure 4.3	Rejection rate, which is the proportion of trials where the null hypothesis is rejected, in the main simulation study. The red, green, and blue bars represent the BHM method, the independent approach, and the proposed method, respectively. Scenarios A1 to A5 vary regarding the number of effective/ineffective treatments.	14
Figure 5.1	Early stopping rate when the prior distribution of one hyperparameter is changed. The red, green, and blue bars represent the BHM method, the independent approach, and the proposed method, respectively. Scenarios B1 to B5 vary regarding the number of effective/ineffective treatments.	17
Figure 5.2	Rejection rate, which is the proportion of trials where the null hypothesis is rejected when the prior distribution of one hyperparameter is changed. The red, green, and blue bars represent the BHM method, the independent approach, and the proposed method, respectively. Scenarios B1 to B5 vary regarding the number of effective/ineffective treatments.	18

Figure 5.3	Early stopping rate when the number of cancer types increases. The red, green, and blue bars represent the BHM method, the independent approach, and the proposed method, respectively. Scenarios C1 to C3 vary regarding the number of effective/ineffective treatments.	20
Figure 5.4	Rejection rate, which is the proportion of trials where the null hypothesis is rejected when the number of cancer types increases. The red, green, and blue bars represent the BHM method, the independent approach, and the proposed method, respectively. Scenarios C1 to C3 vary regarding the number of effective/ineffective treatments.	21
Figure 5.5	Early stopping rate when the number of cancer types increases, and the prior distribution of one hyperparameter is changed. The red, green, and blue bars represent the BHM method, the independent approach, and the proposed method, respectively. Scenarios D1 to D3 vary regarding the number of effective/ineffective treatments.	23
Figure 5.6	Rejection rate, which is the proportion of trials where the null hypothesis is rejected, when the number of cancer types increases, and the prior distribution of one hyperparameter is changed. The red, green, and blue bars represent the BHM method, the independent approach, and the proposed method, respectively. Scenarios D1 to D3 vary regarding the number of effective/ineffective treatments.	24

is a need to incorporate biomarker measurements when classifying the cancer types into subgroups with different efficacy. There are some clinical trial designs which incorporate biomarkers as classifiers which can help to classify cancer types into different subgroups. Takeda et al. (2022 [TLR22]) proposed a Bayesian subgroup design where the cancer types are classified into subgroups according to both the cancer type itself and a second classifier (biomarker). Liu et al. (2023 [LTR23]) also proposed a two-stage design where only patients whose biomarkers measured in the first stage are positive are enrolled in the second stage. These studies highlight the importance of biomarkers as a potential classifier for cancer types because higher values in some biomarkers can be associated with better clinical outcomes. Yin et al. (2021 [Yin+21]) proposed a method that combines finding the biomarker cutoff and testing the effectiveness of the treatment using Bayesian hierarchical modelling. However, these three designs only allow measuring the biomarker one time instead of allowing longitudinal biomarker measurements, and their endpoints are binary instead of continuous.

Longitudinal biomarkers are biomarkers that are collected multiple times over time during the clinical study, which can be used to track the progression and predict the outcome of the disease. Some clinical trials utilize longitudinal biomarker measurements to help predict the outcome of the disease. van Delft et al. (2022 [van+22]) conducted research in which serum tumor marker measurements, which are longitudinal biomarkers, are used to predict the immunotherapy non-response in patients with non-small cell lung cancer. However, this study did not consider classifying more than one cancer type into subgroups. Some clinical studies demonstrate longitudinal biomarkers are associated with a certain clinical outcome. Wu et al. (2017[Wu+17]) found that there is a longitudinal association between fasting blood glucose, which is a type of biomarker, and arterial stiffness risk in non-diabetic individuals. Paulo et al. (2020[Pau+20]) found that a longitudinal increase of HbA1c was independently associated with higher rates of cardiovascular events in patients with type 2 diabetes and multivessel CAD, where HbA1c is a biomarker.

In some clinical trials, researchers are more interested in the progression-free survival time (PFS) instead of the binary indicator of whether the treatment is effective. Consequently, there is a need to develop a clinical trial method that evaluates the effectiveness of a treatment for cancers for which the endpoint is progression-free survival time (PFS) instead of a binary endpoint.

We propose the basket trial design to test the effectiveness of a specific new treatment for several types of cancers for which the endpoint is the survival time. Unlike traditional studies which treat each type of cancer separately, we use Bayesian subgroup analysis to first classify the cancer types into different clusters according to both the survival time and the biomarker measurements of the patients, and then estimate the parameters to find out whether the treatment is effective for each cluster of cancer types. We conclude that the treatment is effective for a cluster of cancer types if the estimated median survival time for this cluster is greater than the threshold that we desire.

In summary, our proposed clinical trial design has many advantages. First, we incorporate the longitudinal biomarker measurements along with the survival outcomes to help classify the cancer

Chapter 2

Methods

2.1 Model

In this study, we consider I types of cancer. For each type of cancer, we recruit n_i patients. We measure the biomarker for each patient L -times, where the measurement times are denoted by t_1, \dots, t_L . The biomarker measurement of the j -th patient in the i -th cancer type measured at time t_l is denoted by Z_{ijl} . We assume that we will measure the biomarker at the same time points for all patients. After we complete the biomarker measurements, we measure the survival time for each patient, denoted by t_{ij} . Let c_{ij} be the censoring indicator for the j -th patient in the i -th cancer type, where $c_{ij} = 1$ if the patient is not censored, and $c_{ij} = 0$ if the patient is censored. We assume that the I types of cancer can be grouped into K clusters according to the biomarker measurements and the survival time. In this article, we consider the case where $K = 2$, which means that there is one effective cluster and one ineffective cluster. However, the method can be generalized for the cases where $K > 2$. The objective of the study is to determine whether the treatment is effective for each cluster of patients, which is reflected by the median survival time for each cluster of patients. The hypothesis test is

$$H_0: \mu_i < q_0 \text{ versus } H_a: \mu_i > q_1,$$

where μ_i is the median survival time for cluster i , q_0 is the median survival time cutoff under which the treatment is deemed ineffective, and q_1 is the median survival time cutoff over which the treatment is deemed effective.

Let π_{ik} denote the probability that cancer type i belongs to cluster k . Let C_i be an indicator of which cluster the cancer type belongs to. For example, $C_1 = 2$ means that the first cancer type belongs to the second cluster. We assume that C_i has the multinomial distribution:

$$C_i \sim \text{Multinomial}(\pi_1, \dots, \pi_K).$$

Recall that Z_{ijl} is the biomarker measurement of the j -th patient in the i -th cancer type measured at time t_l . We assume the biomarker measures are structured as follows,

$$Z_{ij}(C_i = k) = \mu_k(t_j) + v_i + w_{ij} + \epsilon_{ijl},$$

which reflects the grouping structure of the model. Specifically, every cluster has a mean trajectory of the biomarker, which is denoted by $\mu_k(t_j)$. Every group within the cluster can have a mean trajectory that varies from the mean trajectory of the cluster, and the difference is denoted by

$$2 \sim \text{IG}(10^{-3}, 10^{-3}).$$

$$2 \sim \text{Uniform}(-1, 1).$$

$$\sim \text{Gamma}(0.1, 0.1).$$

$$r \sim \text{Gamma}(0.1, 0.1).$$

In the distributions above, $\text{IG}(\cdot, \cdot)$ denotes the inverse Gamma distribution with shape parameter and scale parameter .

2.3 Trial Design

This trial has M planned interim analyses. Let D_m be the observed data at the m -th interim analysis. Recall that t_i is the median survival time for cluster i .

If $P(t_i > (q_0 + q_1)/2 | D_m) < Q_f$, then stop recruiting patients for cancer types that belong to the i -th cluster and conclude that the treatment is ineffective for these types of cancers. Otherwise, continue to recruit patients for these cancer types. Here, Q_f is a probability cutoff; in this study, we set Q_f to be a small value, e.g., 0.05.

At the end of the study, declassified 9t -340(theTd 936(b)-27(elongr]TJ/F49 74(median)-33152 7.9701 Tf 8.624 -1.7

Chapter 3

Illustration

We illustrate how to implement our proposed design using a hypothetical clinical trial. Suppose we would like to evaluate whether a new drug is effective for each of the 12 types of cancers which share the same molecular aberration. Suppose the maximum number of patients in each cancer type is 50, and we have one planned interim analysis. In the first stage, we only recruit 30 patients for each cancer type. We first measure the biomarkers for each patient 20 times. After that, we record the observed survival time and censoring status of each patient.

After we collect the data, we fit the model and sample from the posterior distributions of the parameters. Recall that the interim stopping rule is that if $Pf_i > (q_0 + q_1)/2jD_{mg} < Q_f = 0.05$, then we stop recruiting patients for cancer types which belong to the i -th cluster, and conclude that the treatment is ineffective for these types of cancers. The posterior distribution of β_1 and β_2 are shown below.

The posterior probabilities are $P(C_1 = 1) = P(C_2 = 1) = P(C_3 = 1) = P(C_4 = 1) = P(C_5 = 1) = P(C_6 = 1) = 1$, and $P(C_7 = 1) = P(C_8 = 1) = P(C_9 = 1) = P(C_{10} = 1) = P(C_{11} = 1) = P(C_{12} = 1) = 0$, which means that cancer type 1, 2, 3, 4, 5, 6 belong to the first cluster, and cancer type 7, 8, 9, 10, 11, 12 belong to the second cluster. Since $Pf_1 > (q_0 + q_1)/2jD_{mg} = 0 < Q_f$, we declare that the treatment is ineffective for all the cancer types that are classified into the first cluster.

Since $Pf_2 > (q_0 + q_1)/2jD_{mg} = 0.984 > Q_f$, we continue to recruit 20 more patients for each of the cancer types that are classified into the second cluster, and record the observed survival time and censoring status of each patient in these cancer types. In the second stage, we only use the data of the cancer types that are classified into the second cluster in the previous stage. After that, we fit the model again and estimate the posterior distribution of the parameters again. Recall that at the end of the study, we declare that the treatment is effective if $Pf_i > (q_0 + q_1)/2jD_{mg} > Q$ for the i -th cluster of patients. The posterior distribution of β_1 is shown below.

The posterior probabilities show that $P(C_7 = 1) = P(C_8 = 1) = P(C_9 = 1) = P(C_{10} = 1) = P(C_{11} = 1) = P(C_{12} = 1) = 1$, which means that cancer type 7, 8, 9, 10, 11, 12 are classified into

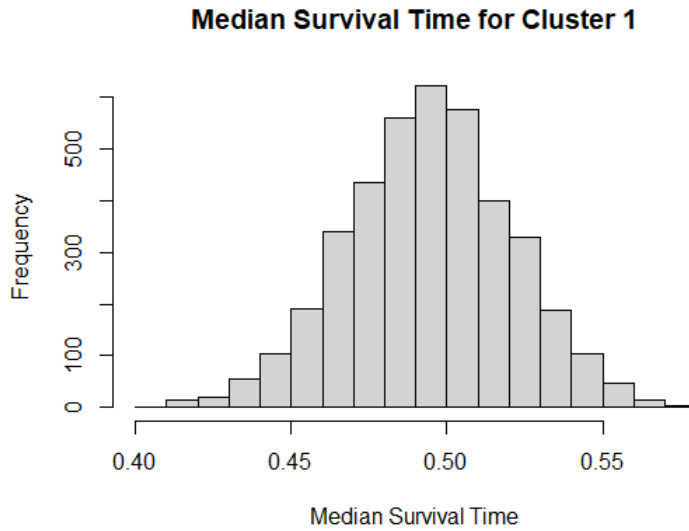


Figure 3.1: The posterior distribution of the median survival time for cluster 1 at the interim analysis.

the first cluster in this stage. Since $Pf_1 > (q_0 + q_1)/2jD_mg = 0.999$, we declare that the treatment is effective for all these six cancer types.

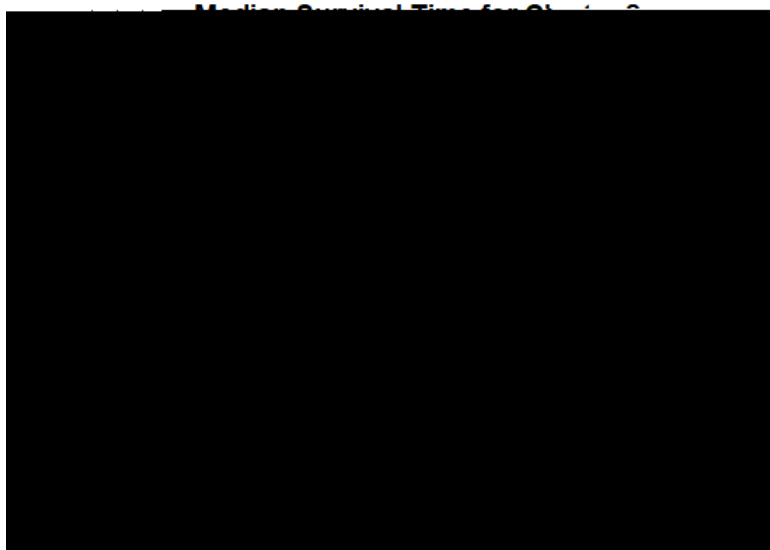


Figure 3.2: The posterior distribution of the median survival time for cluster 2 at the interim analysis.

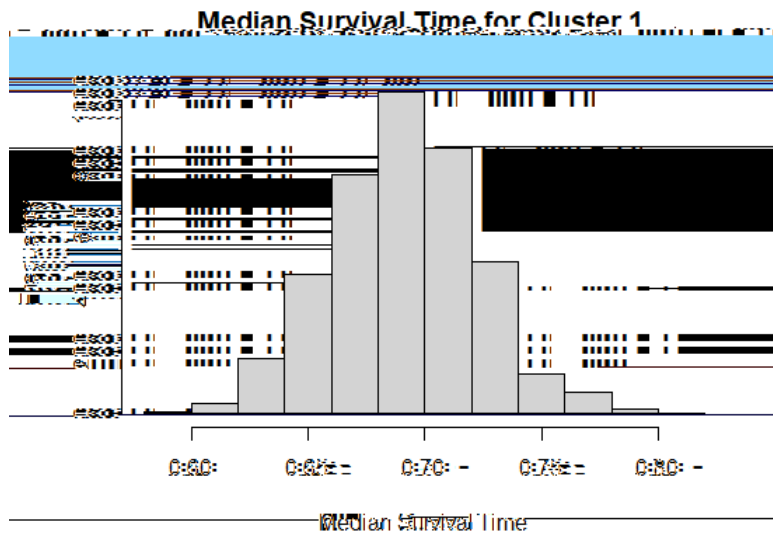


Figure 3.3: The posterior distribution of the median survival time for cluster 1 at the end of the trial.

Chapter 4

Simulation Study

We conduct a simulation study to evaluate the performance of the proposed design. We assume that the cancer types can be grouped into two clusters. The first cluster is the group where the treatment is ineffective, and the second cluster is the group where the treatment is effective. Let

q

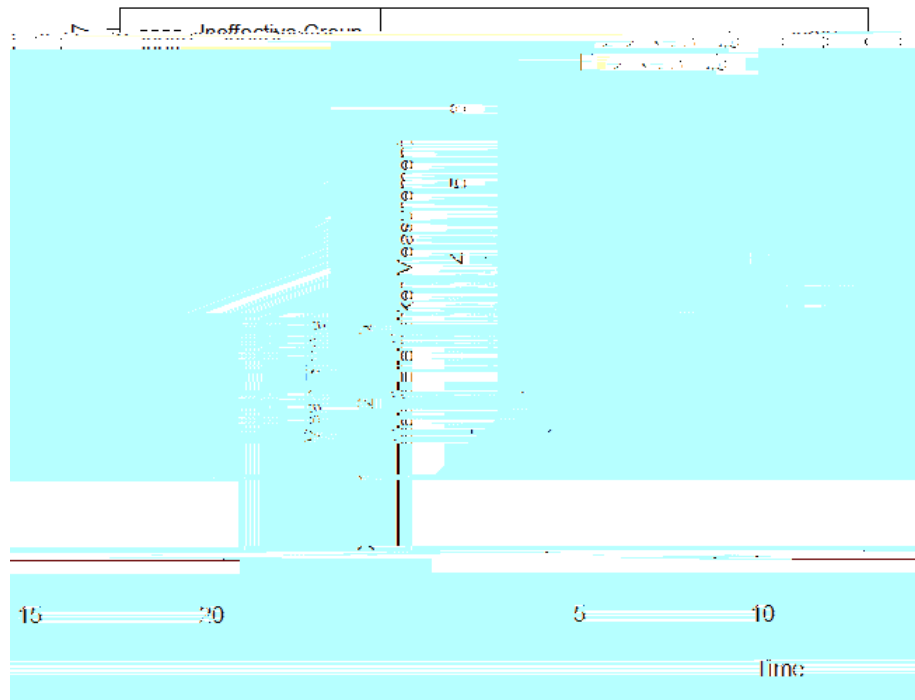


Figure 4.1: Mean biomarker measurement. The solid and dashed line represents the mean biomarker measurement for the effective group and the ineffective group, respectively.

is stopped for this cancer type after the interim analysis because the treatment is considered to be ineffective. If the trial is stopped early for a cancer type, then no new patients will be recruited for this cancer type. Reject means that the null hypothesis is rejected for this cancer type, and we conclude that the treatment is effective for this cancer type. No-Reject means that the trial is not early stopped and the null hypothesis is not rejected after interim 2. Sample Size means the average number of patients that are recruited in each cancer type, which are averaged over the cluster. In scenario A1, there are 12 effective cancer types and no ineffective cancer types. The early stopping rate for the effective group using our proposed model (0.0%) is lower than that using the independent approach (0.7%) or the BHM method (1.6%), which means that fewer patients who are actually in the effective group are wrongly stopped being recruited using our proposed model. The rejection rate for the effective group after interim 2 using our proposed model (99.6%) is higher than that using the independent approach (70.5%) or the BHM (73.6%) method, which means that

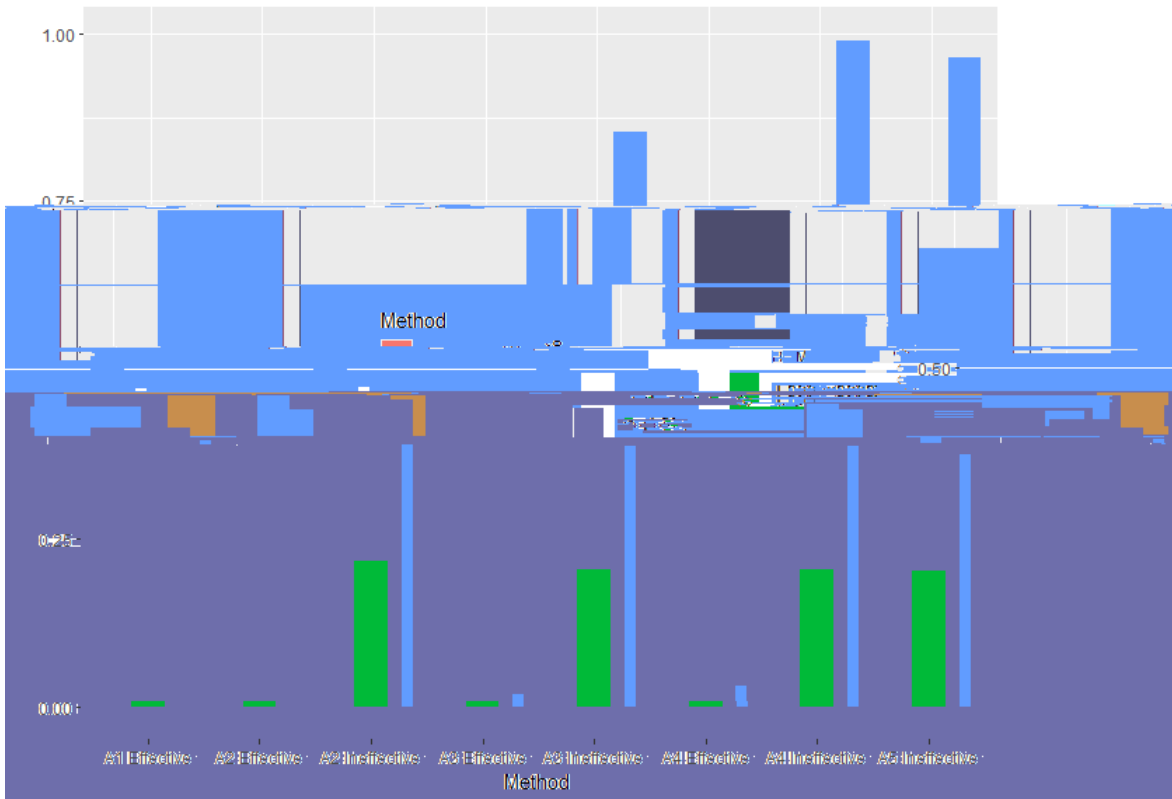


Figure 4.2: Early stopping rate in the main simulation study. The red, green, and blue bars represent the BHM method, the independent approach, and the proposed method, respectively. Scenarios A1 to A5 vary regarding the number of effective/ineffective treatments.

the BHM method and the independent approach. The early stopping rate for the effective group using our proposed model (1.7%) is only slightly higher than that using the independent approach (0.7%) and is lower than that using the BHM method (1.9%). The rejection rate for the effective group after interim 2 using our proposed model (92.5%) is higher than that using the independent approach (63.3%) or the BHM (69.7%) method, which indicates that our proposed method yields much higher power than the other two methods. Again, the reason why our proposed model per-

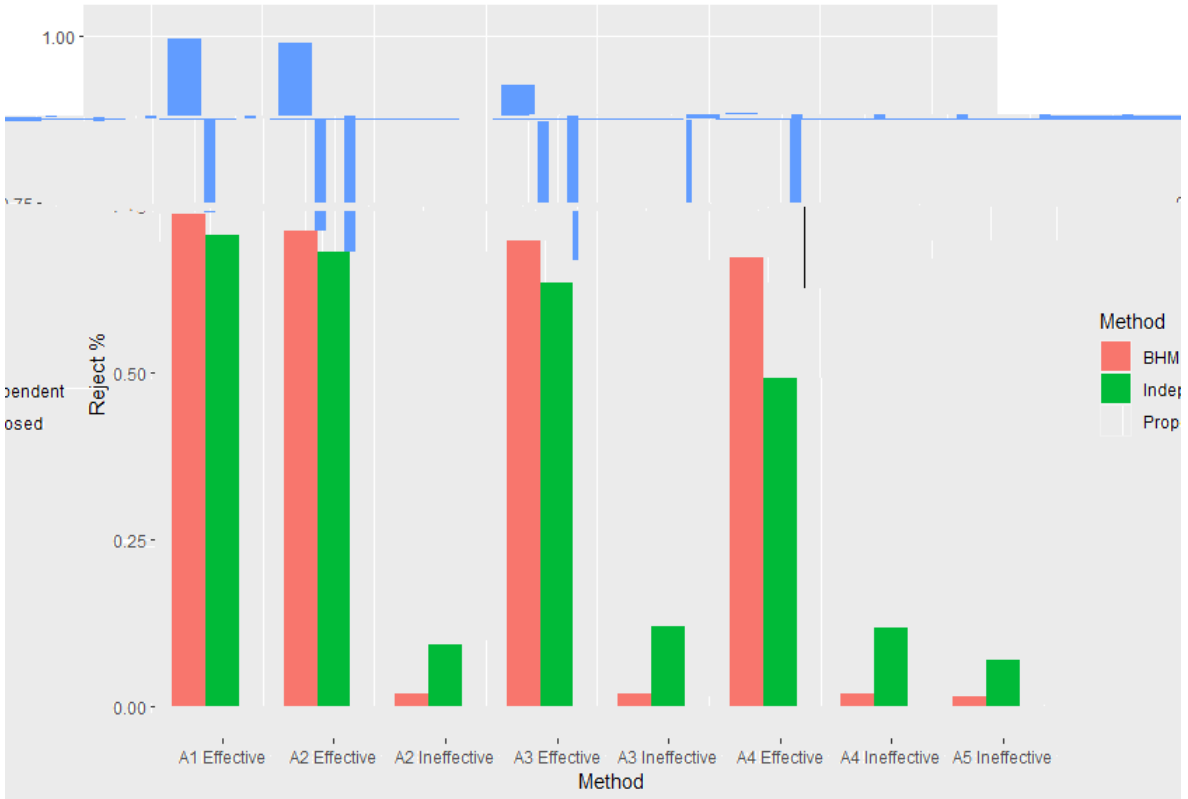


Figure 4.3: Rejection rate, which is the proportion of trials where the null hypothesis is rejected, in the main simulation study. The red, green, and blue bars represent the BHM method, the independent approach, and the proposed method, respectively. Scenarios A1 to A5 vary regarding the number of effective/ineffective treatments.

rate for the effective group, higher rejection rate for the effective group, and lower rejection rate for the ineffective group.

Chapter 5

Sensitivity Analysis

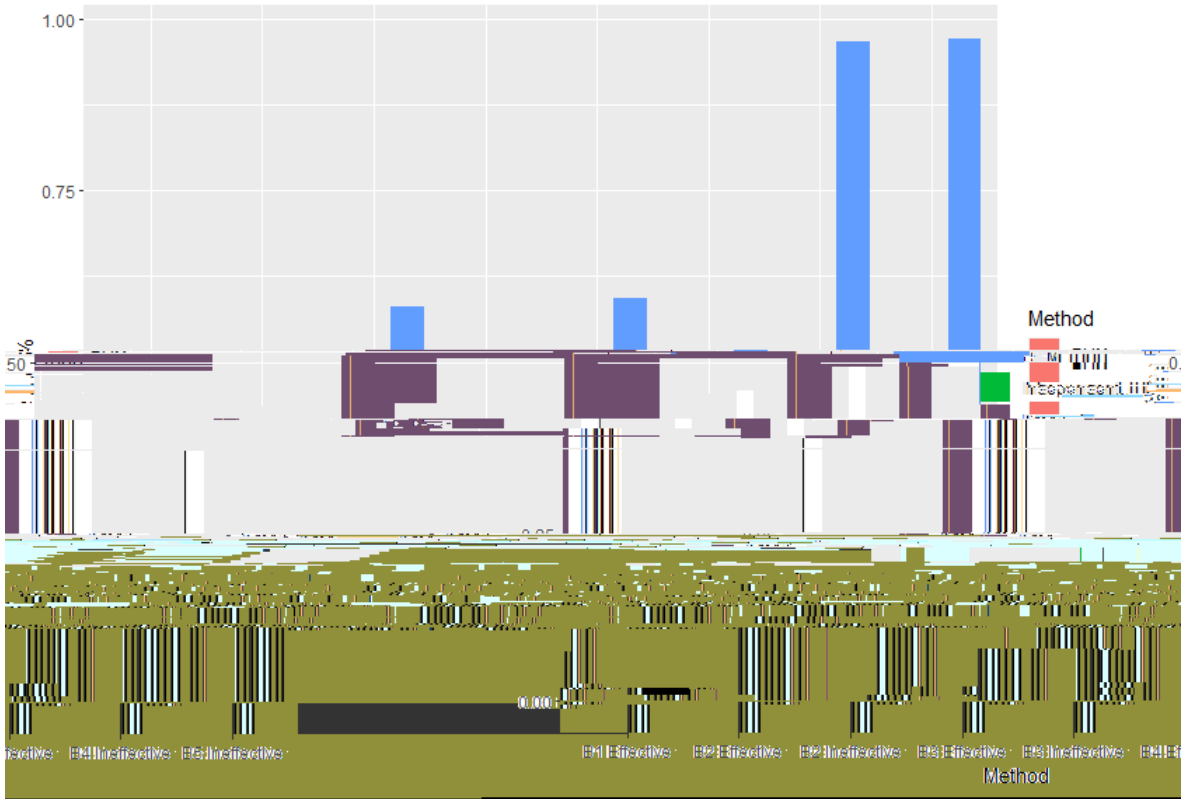


Figure 5.1: Early stopping rate when the prior distribution of one hyperparameter is changed. The red, green, and blue bars represent the BHM method, the independent approach, and the proposed method, respectively. Scenarios B1 to B5 vary regarding the number of effective/ineffective treatments.

C1, C2, and C3, the number of ineffective cancer types is 5, 9, and 18, respectively, and the number of effective cancer types is 13, 9, and 0, respectively. In these three scenarios, our proposed model performs better than the other two methods in general in terms of the early stopping rate and the rejection rate. For example, in scenario C2, the early stopping rate for the ineffective group using our proposed model (89.4%) is higher than that using the independent approach (20.1%) or the BHM method (43.4%). The rejection rate for the ineffective group after interim 2 using our proposed model (0.4%) is lower than that using the independent approach (12.2%) or the BHM method (1.9%). The rejection rate for the effective group after interim 2 using our proposed model (93.0%) is higher than that using the independent approach (64.0%) or the BHM (69.0%) method. The only aspect in this scenario where our proposed model performs worse is that the early stopping rate for the effective group using our proposed model (1.8%) is higher than that using the independent approach (0.5%) and is only slightly lower than that using the BHM (2.2%) method. This simulation study shows that our proposed method performs greatly even if we increase the number of cancer types.

Figure 5.2: Rejection rate, which is the proportion of trials where the null hypothesis is rejected when the prior distribution of one hyperparameter is changed. The red, green, and blue bars represent the BHM method, the independent approach, and the proposed method, respectively. Scenarios B1 to B5 vary regarding the number of effective/ineffective treatments.

In the third sensitivity analysis, we increase the number of cancer types from 12 to 18 and change the prior distribution of σ_2 from Uniform(-1,1) to Uniform(-2,0), so that we can evaluate the performance of the model when there are more cancer types and the prior distribution of one hyperparameter is changed.

Table 5.3 shows the results of the simulation study of the third sensitivity analysis. In scenario D1, D2, and D3, the number of ineffective cancer types is 5, 9, and 18, respectively, and the number of effective cancer types is 13, 9, and 0, respectively. In most cases, our proposed model outperforms the other two methods in terms of the early stopping rate and rejection rate. For example, in scenario D1, The early stopping rate for the ineffective group using our proposed model (75.4%) is higher than that using the independent approach (19.3%) or the BHM method (39.5%). The early stopping rate for the effective group using our proposed model (0.0%) is lower than that using the independent approach (0.5%) or the BHM method (2.0%). The rejection rate for the effective

			Early Stop %	Reject %	No-Reject %	Sample Size
C1	Proposed Model	Ine ective	82.2	4.8	13.0	33.6
		E ective	0.0	98.4	1.6	50.0
	Independent Approach	Ine ective	19.3	10.5	70.2	46.1
		E ective	0.5	68.8	30.7	49.9
	BHM	Ine ective	39.5	1.8	58.7	42.1
		E ective	2.0	70.8	27.3	49.6
C2	Proposed Model	Ine ective	89.4	0.4	10.2	32.1
		E ective	1.8	93.0	5.2	49.6
	Independent Approach	Ine ective	20.1	12.2	67.7	46.0
		E ective	0.5	64.0	35.5	49.9
	BHM	Ine ective	43.4	1.9	54.7	41.3
		E ective	2.2	69.0	28.8	49.6
C3	Proposed Model	Ine ective	97.3	0.0	2.7	30.5
		E ective	-	-	-	-
	Independent Approach	Ine ective	20.3	7.5	72.2	45.9
		E ective	-	-	-	-
	BHM	Ine ective	51.7	1.6	46.7	39.7
		E ective	-	-	-	-

Table 5.2: Simulation results of the sensitivity analysis when the number of cancer types increases. This table shows the early stopping rate, rejection rate, and sample size under three simulation scenarios.

group after interim 2 using our proposed model (96.8%) is higher than that using the independent approach (68.8%) or the BHM (70.8%) method. The only drawback to our proposed model in this scenario is that the rejection rate for the ine ective group after interim 2 using our proposed model (10.2%) is only slightly lower than that using the independent approach (10.5%) and is higher than that using the BHM (1.8%) method.

In summary, our proposed model still performs better in most of the scenarios, which means that the model is not very sensitive to the number of cancer types or the prior distribution of the hyperparameter.

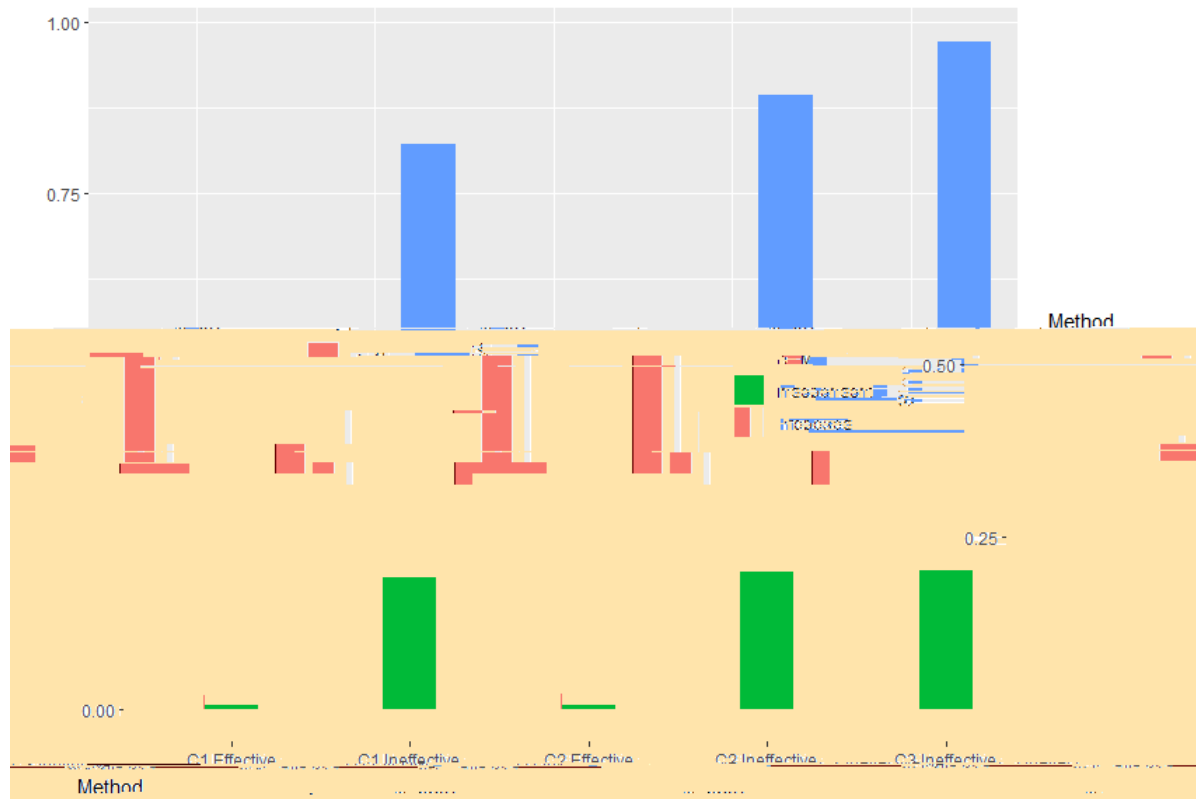


Figure 5.3: Early stopping rate when the number of cancer types increases. The red, green, and blue bars represent the BHM method, the independent approach, and the proposed method, respectively. Scenarios C1 to C3 vary regarding the number of effective/ineffective treatments.

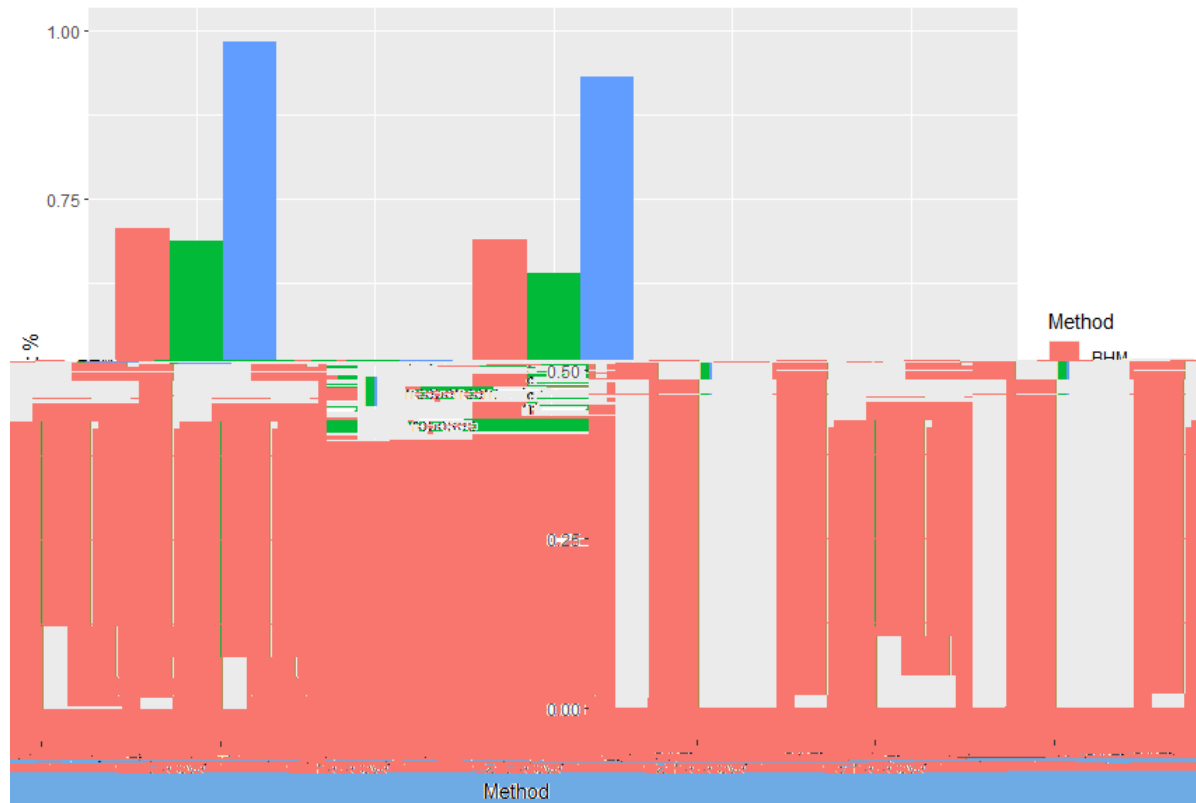


Figure 5.4: Rejection rate, which is the proportion of trials where the null hypothesis is rejected when the number of cancer types increases. The red, green, and blue bars represent the BHM method, the independent approach, and the proposed method, respectively. Scenarios C1 to C3 vary regarding the number of effective/ineffective treatments.

			Early Stop %	Reject %	No-Reject %	Sample Size
D1	Proposed Model	Ineffective	75.4	10.2	14.4	34.9
		Effective	0.0	96.8	3.2	50.0
	Independent Approach	Ineffective	19.3	10.5	70.2	46.1
		Effective	0.5	68.8	30.7	49.9
	BHM	Ineffective	39.5	1.8	58.7	42.1
		Effective	2.0	70.8	27.3	49.6
D2	Proposed Model	Ineffective	73.4	1.4	25.2	35.3
		Effective	6.4	77.5	16.1	48.7
	Independent Approach	Ineffective	20.1	12.2	67.7	46.0
		Effective	0.5	64.0	35.5	49.9
	BHM	Ineffective	43.4	1.9	54.7	41.3
		Effective	2.2	69.0	28.8	49.6
D3	Proposed Model	Ineffective	97.9	0.0	2.1	30.4
		Effective	-	-	-	-
	Independent Approach	Ineffective	20.3	7.5	72.2	45.9
		Effective	-	-	-	-
	BHM	Ineffective	51.7	1.6	46.7	39.7
		Effective	-	-	-	-

Table 5.3: Simulation results of the sensitivity analysis when the number of cancer types increases, and the prior distribution of one hyperparameter is changed. This table shows the early stopping rate, rejection rate, and sample size under three simulation scenarios.

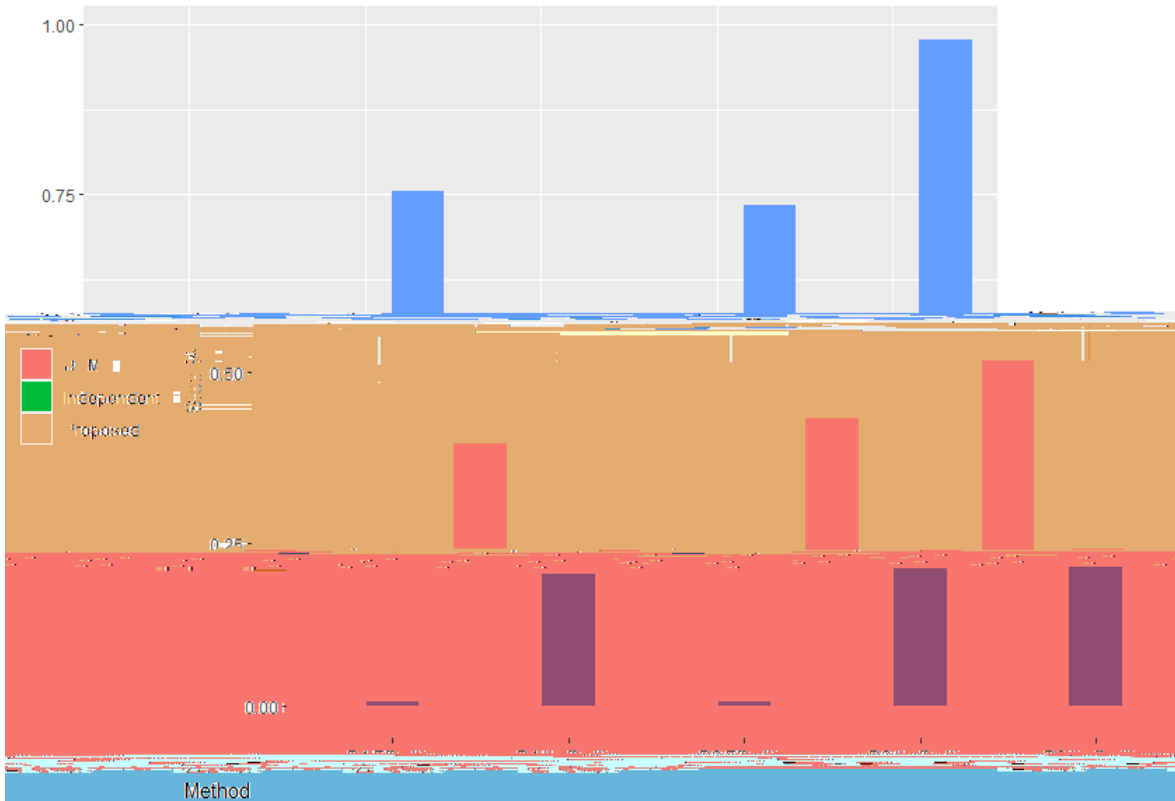


Figure 5.5: Early stopping rate when the number of cancer types increases, and the prior distribution of one hyperparameter is changed. The red, green, and blue bars represent the BHM method, the independent approach, and the proposed method, respectively. Scenarios D1 to D3 vary regarding the number of effective/ineffective treatments.

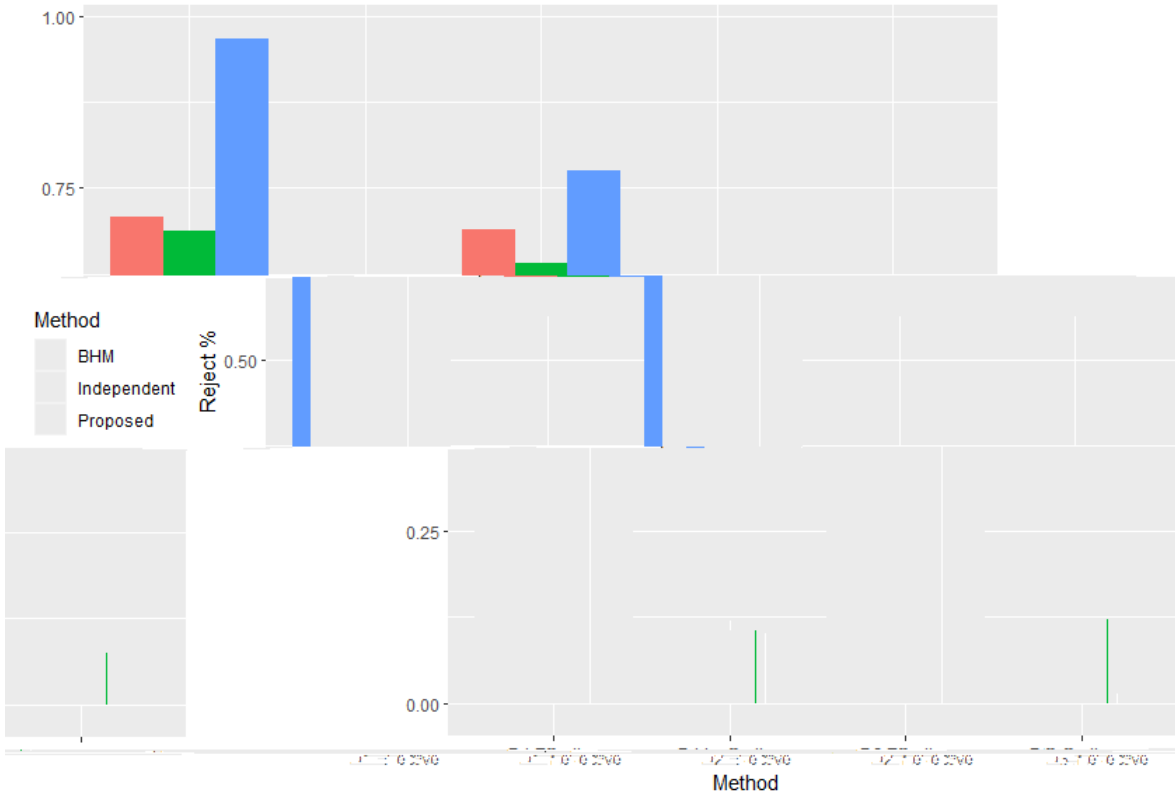


Figure 5.6: Rejection rate, which is the proportion of trials where the null hypothesis is rejected, when the number of cancer types increases, and the prior distribution of one hyperparameter is changed. The red, green, and blue bars represent the BHM method, the independent approach, and the proposed method, respectively. Scenarios D1 to D3 vary regarding the number of effective/ineffective treatments.

Chapter 7

Gibbs Sampler for the Proposed Model

Step 1: We update C_i .

We denote $Z_{ij} = (Z_{ij1}, \dots, Z_{ijL})$, and $Z_i = (Z_{i1}, \dots, Z_{iJ})$. For $i = 1, \dots, I$, $C_i \sim \text{Multinomial}(n_i, \dots, iK)$, where

$$iK = \frac{\prod_{i=1}^K N_{Q_i}(u_{i(k)}, \Sigma_{Q_i}) \prod_j [f_i(t_{ij})g^{1-ij} f_S(t_{ij})g^{1-ij}]}{\prod_{i=1}^K N_{Q_i}(u_{i(k)}, \Sigma_{Q_i}) \prod_j [f_i(t_{ij})g^{1-ij} f_S(t_{ij})g^{1-ij}]},$$

where $u_{i(k)} = X_{i \cdot} z_{i(k)} + X_{i \cdot b} \mathbf{b}_i$, $Q_i = Ln_i$,
 $z_{i(k)} = (z_{i1(k)}, z_{i2(k)}, \dots, z_{iS(k)})^T$,
 $\mathbf{b}_i = (v_i, w_{i1}, \dots, w_{iJ})^T$.

Here, $N_{Q_i}(w, \Sigma_{Q_i})$ is a Q_i -variate normal density function of Z_i , $X_{i \cdot}$ is a Q_i -by- S design matrix of the i -th arm associated with $z_{i(k)}$, and $X_{i \cdot b}$

Normal distributions, and the prior distributions are $\frac{2}{v} \text{IG}(10^{-3}, 10^{-3})$, $\frac{2}{w} \text{IG}(10^{-3}, 10^{-3})$, and $\frac{2}{j} \text{IG}(10^{-3}, 10^{-3})$, we are calculating the posterior distribution of the variance of the Normal distribution where the mean is known and the prior distribution of the variance follows Inverse Gamma distribution. As a result, we get the posterior distributions.

$$\begin{aligned} \frac{2}{v} & \text{IG}(10^{-3} + 0.5I, 10^{-3} + 0.5 \prod_{i=1}^I \prod_{j=1}^{n_j} v_i^2), \\ \frac{2}{w} & \text{IG}(10^{-3} + 0.5N, 10^{-3} + 0.5 \prod_{i=1}^I \prod_{j=1}^{n_j} w_{ij}^2), \\ \frac{2}{j} & \text{IG}(10^{-3} + 0.5LN, 10^{-3} + 0.5 \prod_{i=1}^I \prod_{j=1}^{n_j} \prod_{l=1}^L \frac{2}{ij}). \end{aligned}$$

and $X_{b(k)}$ is a Q_k -by- $(I + N)$ matrix. The values of $q^{(k)}$ for each cluster k , where each column corresponds to one of v_i and w_{ij} for each observation in cluster k , where each row corresponds to one of v_i and w_{ij} . Since $Z_{ij}j(C_i = k) = \mu_k(t_i)$, we use the matrix notation from the previous section to get that $\mu_k(t_i) = \sum_{j=1}^J Z_{ij} \beta_j$. At this step, we are calculating the posterior mean of β_j for each variable where the variance is σ_j^2 of β_j . Since the prior distribution of β_j is $N(\mu_j, \sigma_j^2)$, we can use β_j using exactly the same method as in the previous section.

In summary, the full conditional distribution of β_j is

Step 6: We update β_j using a Uniform distribution $U(-1, 1)$.

with the random-effect vector β_j (one for each patient) and σ_j^2 (one for each observation in the dataset). We use the B-Spline basis functions β_j for each patient) are stored in the dataset for each observation in the dataset for each patient. We use the matrix notation $\beta_j = (\beta_{j1}, \dots, \beta_{jI})^T$. When we use the mean of a multivariate normal distribution, the variance matrix of the posterior distribution can be derived as follows:

$$\sigma_j^2 = \text{diag}(\sigma_j^2, \dots, \sigma_j^2)^{-1},$$

$$\mu_j = X_{b(k)} \beta_j.$$

It follows, where

ing. Since the prior distribution of β_j is $N(\mu_j, \sigma_j^2)$, we can use the same method as in the previous section. (Step) -542(6.) -543(W) (up) -28(

$$f(r_j) / f_{\text{gamma}}(r, 0.1, 10)^Q \prod_{ij} [f_{f_t}(t_{ij})g^{\eta} f_{S_t}(t_{ij})g^{1-\eta}],$$

where $f_{\text{gamma}}(x, \eta, \lambda)$ is the probability density function of a Gamma random variable where the shape is η and the rate is λ .

Chapter 8

Model Specification and Gibbs Sampler for the BHM

The structure of the Bayesian Hierarchical Model is as follows. The survival function for the i -th patient in the j -th cancer type is related to the cancer type of the patient in the following way, where μ_j , σ_j^2 , and r_j are the parameters corresponding to each cancer type.

$$S_i(t_{ij}) = \exp\left\{-\frac{r_j}{t_{ij}} \exp(\mu_j)\right\}$$

We assume the parameters have the distributions, where μ_j , σ_j^2 , α_j , β_j , r_j , and γ_j are the hyperparameters.

$$\begin{aligned} \mu_j &\sim N(\mu, \sigma^2), \\ \sigma_j^2 &\sim \text{Gamma}(\alpha, \beta), \\ r_j &\sim \text{Gamma}(\gamma, \delta). \end{aligned}$$

We assume the hyperparameters have the prior distributions.

$$\begin{aligned} \mu &\sim N(0, 10), \\ \sigma^2 &\sim \text{Unif}(0, 10), \\ \alpha &\sim \text{Unif}(0, 1), \\ \beta &\sim \text{Unif}(0, 1), \\ \gamma &\sim \text{Unif}(0, 1), \\ \delta &\sim \text{Unif}(0, 1). \end{aligned}$$

The Gibbs sampler is as follows.

Step 1: We update μ_j , σ_j^2 , and r_j using Metropolis sampling

$$f(\mu_j) \propto \frac{1}{\sigma_j^2} \exp\left\{-\frac{\mu_j^2}{\sigma_j^2}\right\} \prod_j [f_j(t_{ij})] \exp\left\{-\frac{r_j}{t_{ij}} \exp(\mu_j)\right\} \times \text{Unif}(0, 1)$$

where $f_N(x, \mu, \sigma)$ is the probability density function of a Normal(μ, σ) random variable where the mean is μ and the standard deviation is σ , and $f_{gamma}(x, \alpha, \beta)$ is the probability density function of a Gamma random variable where the shape is α and the rate is β . Here, $f_t(t_{ij})$ is the probability density function of PFS of the i -th patient in the j -th cancer type, and $S_t(t_{ij})$ is the survival function of PFS of the i -th patient in the j -th cancer type.

Step 2: We update $\mu, \sigma^2, \alpha, \beta, r_1$, and r_2 using Metropolis sampling

$$f(\mu, \sigma^2, \alpha, \beta, r_1, r_2) / f_N(\mu, \sigma^2, 0, 10) f_{gamma}(\alpha, \beta, x)$$

Bibliography

- [CL20] Nan Chen and J Jack Lee. Bayesian cluster hierarchical model for subgroup borrowing in the design and analysis of basket trials with binary endpoints . In: *Statistical Methods in Medical Research* 29.9 (2020). PMID: 32178585, pp. 2717-2732. doi : 10.1177/0962280220910186 eprint: <https://doi.org/10.1177/0962280220910186> .
url : <https://doi.org/10.1177/0962280220910186> .
- [CY18] Yiyi Chu and Ying Yuan. BLAST: Bayesian latent subgroup design for basket trials

lib.sfu.ca/login?url=https://www.proquest.com/scholarly-journals/association-longitudinal-values-glycated/docview/2668181506/se-2

- [Sam+19] Robert M. Samstein et al. Tumor mutational load predicts survival after immunotherapy across multiple cancer types . In: *Nature Genetics* 51.2 (Feb. 2019), pp. 202-206. issn: 1546-1718. doi : 10.1038/s41588-018-0312-8 . url : <https://doi.org/10.1038/s41588-018-0312-8> .
- [TLR22] Kentaro Takeda, Shufang Liu, and Alan Rong. Constrained hierarchical Bayesian model for latent subgroups in basket trials with two classes . In: *Statistics in Medicine* 41.2 (2022), pp. 298-309. doi : <https://doi.org/10.1002/sim.9237> . eprint: <https://onlinelibrary.wiley.com/doi/pdf/10.1002/sim.9237> . url : <https://onlinelibrary.wiley.com/doi/abs/10.1002/sim.9237> .
- [van+22] Frederik A. van Delft et al. Modeling strategies to analyse longitudinal biomarker data: An illustration on predicting immunotherapy non-response in non-small cell lung cancer . In: *Heliyon* 8.10 (2022), e10932. issn: 2405-8440. doi : <https://doi.org/10.1016/j.heliyon.2022.e10932> . url : <https://www.sciencedirect.com/science/article/pii/S2405844022022204> .
- [Wu+17] Yuntao Wu et al. Longitudinal fasting blood glucose patterns and arterial stiffness risk in a population without diabetes . English. In: *PLoS One* 12.11 (Nov. 2017). url :